Title: Predictors of radiation dose for uterine artery embolisation are angiography system-dependent

Short running title: UAE RADIATION DOSE PREDICTORS ARE SYSTEM-DEPENDENT

Don J. Nocum[1, 2 *], John Robinson[2, 3], Mark Halaki[4], Magnus Båth[5, 6], John D. Thompson[7], Nadine Thompson[1, 8], Michelle Moscova[9], Eisen Liang[1, 10], Nejc Mekiš[11], Warren Reed[2, 3]

[1] SAN Radiology & Nuclear Medicine, Sydney Adventist Hospital, Wahroonga, New South Wales, Australia
[2] Discipline of Medical Imaging Science, Sydney School of Health Sciences, Faculty of Medicine and Health, The University of Sydney, New South Wales, Australia
[3] Medical Imaging Optimisation and Perception Group (MIOPeG), Discipline of Medical Imaging Science, Sydney School of Health Sciences, Faculty of Medicine and Health, The University of Sydney, New South Wales, Australia
[4] Faculty of Medicine and Health, Sydney School of Health Sciences, Discipline of Exercise and Sports Science, The University of Sydney, New South Wales, Australia
[5] Department of Medical Radiation Sciences, Institute of Clinical Sciences, The Sahlgrenska Academy, University of Gothenburg, Gothenburg SE-413 45, Sweden
[6] Department of Medical Physics and Biomedical Engineering, Sahlgrenska University Hospital, SE-413 45 Gothenburg, Sweden
[7] Department of Radiography, School of Health and Society, University of Salford, Salford, M6 6PU, United Kingdom
[8] School of Medicine, Faculty of Medicine and Health, The University of Sydney, New South Wales, Australia
[9] Faculty of Medicine and Health, School of Medical Sciences, University of New South Wales, Sydney, New South Wales, Australia
[10] Sydney Fibroid Clinic, Sydney Adventist Hospital, Wahroonga, New South Wales, Australia
[11] Medical Imaging and Radiotherapy Department, Faculty of Health Sciences, University of Ljubljana, Ljubljana, Slovenia

***Corresponding author:**
Don J. Nocum
SAN Radiology & Nuclear Medicine
Sydney Adventist Hospital
185 Fox Valley Road
Wahroonga 2076
New South Wales, Australia
Phone: +61 02 9480 9821 Fax: +61 02 9480 9845
Email: donjohnson.nocum@sah.org.au

Conflict of Interest: The authors declare no conflict of interest.

Abstract

This study sought to achieve radiation dose reductions for patients receiving uterine artery embolisation (UAE) by evaluating radiation dose measurements for the preceding generation (Allura) and upgraded (Azurion) angiography system. Previous UAE regression models in the literature could not be applied to this centre's practice due to being based on different angiography systems and radiation dose predictor variables. The aims of this study were to establish whether radiation dose is reduced with the upgraded angiography system and to develop a regression model to determine predictors of radiation dose specific to the upgraded angiography system. A comparison between Group I (Allura, n = 95) and Group II (Azurion, n = 95) demonstrated a significant reduction in KAP (kerma-area product) and Ka, r (reference air kerma) by 63% (143.2 Gy·cm^2 vs 52.9 Gy·cm^2; $P < 0.001$, $d = 0.8$) and 67% (0.6 Gy vs 0.2 Gy; $P < 0.001$, $d = 0.8$), respectively. The multivariable linear regression (MLR) model identified the UAE radiation dose predictors for KAP on the upgraded angiography system as total fluoroscopy dose, Ka, r, and total uterus volume. The predictive accuracy of the MLR model was assessed using a Bland-Altman plot. The mean difference was 0.39 Gy·cm^2 and the limits of agreement (LoA) were +28.49 and -27.71 Gy·cm^2, and thus illustrated no proportional bias. The resultant MLR model was considered system-dependent and validated the upgraded angiography system and its advance capabilities to significantly reduce radiation dose. Interventional radiologist and interventional radiographer familiarisation of the system's features and the implementation of the newly established MLR model would further facilitate dose optimisation for all centres performing UAE procedures using the upgraded angiography system.

Keywords: Bland-Altman plot, dose optimisation, multivariable linear regression, radiation dose, regression model, uterine artery embolisation

1. Introduction

Uterine artery embolisation (UAE) is a well-established, non-surgical treatment for patients with uterine fibroids or adenomyosis, suffering from menorrhagia, dysmenorrhea, bladder compression and other bulk-related symptoms.(1-3) ~~A Cochrane review in 2014 compared this minimally invasive procedure to hysterectomy and myomectomy and found that UAE provided comparable symptom relief and quality of life (QOL) improvement.(4)~~ UAE is currently accepted as an alternative to surgery given its effectiveness to durably improve uterine disease-related symptoms, as well as its tolerability to reduce patient recovery-related pain and discomfort.(4-5) ~~UAE is potentially emerging as a preferred treatment alternative to benign uterine diseases, especially within the Australian context.(6-7)~~

Radiation dose exposure to patients is particularly crucial during moderate to complex angiographically-guided interventional procedures such as UAE. It is the role of the interventional radiologist and interventional radiographer to optimise radiation dose according to the ALARA ('as low as reasonably achievable') principle and minimise the risks of radiation-induced injury.(8) According to the International Commission on Radiological Protection (ICRP) Publication 103, justification of the radiation exposure and an estimation of the radiation risk must be considered.(9) Since most women having UAE are of reproductive age, radio-sensitive organs of the pelvis, especially the ovaries, are exposed to the primary x-ray beam.(8) Hence, radiation dose optimisation is paramount to reduce the risk of tissue reactions (deterministic effects) and stochastic effects.(8) Uterine and fertility preservation are important for women choosing UAE over its surgical alternatives, as recent studies have highlighted that pregnancy post-UAE can been achieved.(10-11)

The Australian Government financially incentivises radiology service providers to regularly replace and to perform major upgrades of angiographic equipment every 10-15 years.(12) ~~In countries where there may be no impetus or funding to upgrade to the latest, radiation-reducing imaging equipment, patients are being exposed to higher and unnecessary radiation doses.(13-14) As our previous system had reached the end of its service life at 10 years, the planned purchase of a new angiography system incorporated dose limiting technology in both the software real-time image processing algorithms and hardware x-ray detection systems.(15) These advancements enable improved features and user functionality in the upgraded angiography system to reduce radiation dose.(16-17) Therefore, the radiation dose exposure is theoretically lower compared to the previous generation of angiography systems.~~ Several studies have demonstrated that practical dose reductions have been attained using similar technology for coronary intervention[17-18], endovascular aortic repairs and aorto-iliac occlusive disease intervention[19], transarterial chemoembolisation[20-21], and neuro diagnostic and interventional angiography[15, 22]. ~~However, the dose comparisons shown in this study between the preceding generation Allura Xper FD20 (Philips Healthcare, Eindhoven, Netherlands) and newly installed Azurion 7 M20 with FlexArm (Philips Healthcare, Eindhoven, Netherlands) have not been previously reported for UAE procedures.~~

Kerma-area product (KAP) is a surrogate measure of the amount of energy delivered to the patient[23] and has been generally described by Kwon et al[24] as an adequate predictor of effective dose. The use of the term 'radiation dose' in this paper refers to different dose-related measures, specifically KAP. In our previous study[25], KAP was used as a reliable predictor outcome variable to identify the predictors of radiation dose for UAE using the Allura Xper FD20. Under these specific conditions, it was found that total DSA (digital subtraction angiography), total CRM (conventional roadmap), and total LIH (last-image hold) dose as a function of the total procedural KAP were the significant radiation dose predictors identified following multivariable linear regression (MLR) analysis.[25] ~~However, the upgraded system no longer records LIH dose or saved fluoroscopy information in contrast to its previous generation.~~ There is a paucity of literature based on the formulation of regression models for UAE[25-27] or the application of the identified radiation dose predictors to optimise UAE practice[28]. Previous UAE regression models[25-27] were based on different angiography systems and sets of radiation dose predictor variables and could not be applied to this study. ~~The new MLR model, was tested for robustness using a Bland-Altman plot, is advantageous for optimising dose in future UAE procedures performed on the upgraded angiography system.~~

~~UAE as a non-surgical alternative treatment for symptomatic fibroids and/or adenomyosis becomes even more appealing when significant radiation dose reduction can be achieved.~~ This is the first known investigation in the Australian context for comparing UAE radiation dosimetry between the upgraded angiography system and its predecessor to determine the magnitude of dose reduction. The aims of this study were to establish whether radiation dose is reduced with an upgraded angiography system and to develop a regression model to determine predictors of radiation dose specific to the upgraded angiography system. The outcomes of this study can be used to maximise radiation dose optimisation at centres performing UAE procedures on the upgraded angiography system.

2. Material and methods

Ethics approval was granted by the Adventist HealthCare Limited Human Research Ethics Committee (AHCL HREC). Informed consent was obtained from all patients in both groups in this study. All patient records and data were de-identified and protected.

2.1 Study Setting

This study was performed in the angiography suite within the radiology department of a teaching hospital. The patient cohorts were treated for symptomatic uterine fibroid and/or adenomyosis using UAE. The interventional radiologist consulted and consented all patients prior to the procedure. Patients were reviewed based on their medical history, including their symptoms, age, prior fibroid therapies, patient's preference regarding uterine sparing therapy (over hysterectomy and myomectomy), plans for future pregnancy, and assessed for possible procedural risks. All patients had undergone a pelvic magnetic resonance imaging (MRI) examination to ensure suitability for the UAE procedure. [(29)] The inclusion criteria for this study were as follows: (1) no previous UAE for the treatment of symptomatic uterine fibroids and/or adenomyosis, and (2) bilateral uterine artery embolisation via a transfemoral approach. The UAE procedure protocol has been described in a study by Liang et al[(1)].

Retrospective data on 95 patients were included in Group I where UAE procedures were performed between July 2018 and August 2019 using the preceding generation angiography system (Philips Allura Xper FD20, Philips Healthcare, Eindhoven, Netherlands). This was compared with 95 prospective patients in Group II where UAE procedures were performed between January to December 2020 using the upgraded angiography system (Philips Azurion 7 M20 with FlexArm, Philips Healthcare, Eindhoven, Netherlands)

Three different types of x-ray imaging modes including DSA, CRM or *navigate* (Philips Healthcare, Eindhoven, Netherlands), and live fluoroscopy, were used at the discretion of the interventional radiologist and interventional radiographer during each UAE procedure. The LIH dose or any saved fluoroscopy information is no longer recorded on the upgraded angiography systems post-procedure dose report. DSA was acquired at a multi-phase acquisition pulsed rate setting of 2 frames per second (fps) for 3 seconds (s), 1 fps for 2 s, and

0.5 fps thereafter. This was changed from the default factory setting for an iliac/pelvis DSA which used a multi-phase setting of 3 fps for 4 s, 1 fps for 8 s, and 0.5 fps thereafter. The fluoroscopy pulsed frequency at the low-dose setting was 7.5 fps, and the medium to high-dose settings were at 15 fps. The fluoroscopy added filters were set at 0.90 mm Cu and 1.00 mm Al.

2.2 Data Collection

Patient demographic and clinical data was collected, including age (years), height (cm), body mass (kg), body mass index (BMI) (kg/m^2), total number of fibroids (*n*), total fibroid volume (cm^3), and total uterus volume (cm^3). Radiation dose measurements that were recorded included the overall KAP ($Gy{\cdot}cm^2$), Ka, r (Gy), and fluoroscopy time (minutes). The Ka, r is the air kerma in the interventional reference point (IRP). The KAP for each imaging mode including total DSA, total CRM, and total fluoroscopy dose ($Gy{\cdot}cm^2$) were also calculated. A calibrated KAP meter (Kerma X-plus, IBA Dosimetry; Schwarzenbruck, Germany) fitted on the exit surface of the collimator assembly was used to measure KAP.

2.3 Statistical Analysis

SPSS Statistics v27 (IBM Corp., Armonk, NY) was used to perform the descriptive statistics for both Group I (Allura, $n = 95$) and Group II (Azurion, $n = 95$). Mean ± standard deviation (M ± SD) scores were calculated since all variables were normally distributed. A paired sample T-test compared the patient demographic and clinical information, and radiation dose measurements between the two patient groups. A *P*-value <0.05 was considered statistically significant. The effect sizes were also calculated and based on Cohen's method, the following criteria were used to evaluate the correlation coefficients: nil ($d < 0.2$), weak ($0.2 \leq d > 0.5$), moderate ($0.5 \leq d < 0.8$) and strong ($d \geq 0.8$).[30]

Bivariate correlations using Pearson's correlations were used for the evaluation of association between KAP and all possible independent predictor variables. A Pearson's correlation matrix was also undertaken to show any significant bivariate correlations between the independent variables included in the regression analysis. An MLR with stepwise elimination[25] was performed using the following predictor variables: BMI, number of fibroids, total fibroid volume, total uterus volume, Ka, r, fluoroscopy time, total DSA dose, total CRM dose, and total fluoroscopy dose. Scatter plots of the predictor variables and KAP were visually checked to confirm the assumption of a linear association between the predictor variables and KAP. The criteria used for the stepwise selection process was based on *P*-values ($P < 0.05$).

A Bland-Altman plot[31] was used to evaluate the predictive accuracy of the MLR model and validity of the identified radiation dose predictor variables by comparing the Predicted KAP with the Actual KAP for Group II. The Difference (Actual KAP – Predicted KAP) and Mean ([Actual KAP + Predicted KAP]/2) were calculated. A one-sample T-test was used to assess the use of a Bland-Altman plot if the *P*-value was not significant ($P > 0.001$). The mean difference and the limits of agreement (LoA) were calculated and depicted on the Bland-Altman plot. The readings were also divided into three different BMI categories ($18.5 \leq$ BMI ≤ 24.9 kg/m^2, $25 \leq$ BMI ≤ 29.9 kg/m^2, and BMI ≥ 30 kg/m^2).

3. Results

Table 1 demonstrates the patient demographic and clinical data from the patients in Group I (Allura; $n = 95$) and Group II (Azurion; $n = 95$).

Out of the 95 patients in Group II, a post-aortogram (following bilateral uterine artery embolisation) was performed in 15 patients, ovarian artery supply (OAS) was investigated in 8 patients, and 7 patients had one or two ovarian arteries embolised due to OAS to the fibroid and/or adenomyosis.

Radiation dose measurements were compared between the Group I (Allura, $n = 95$) and Group II (Azurion; $n = 95$) in Table 2. All variables were statistically significant ($P < 0.01$). The KAP M ± SD was 143.2 ± 115 Gy·cm^2 (median = 115.8 Gy·cm^2) for Group I compared to 52.9 ± 52 Gy·cm^2 (median = 30.6 Gy·cm^2) for Group II ($P < 0.001$, $d = 0.8$), resulting in a 63% dose reduction. The Ka, r M ± SD also showed a 67% reduction in dose, with a Group I 0.6 ± 0.5 Gy (median = 0.4 Gy) versus Group II 0.2 ± 0.2 Gy (median = 0.14 Gy) ($P < 0.001$, $d = 0.8$). The M ± SD fluoroscopy time for Group I was 13.5 ± 6 minutes in contrast to Group II which was 11.6 ± 5 minutes ($P = 0.017$, $d = 0.2$). The total DSA, total CRM, and total fluoroscopy doses in Group II all demonstrated a marked reduction with a M ± SD of 22.9 ± 24 ($P < 0.001$, $d = 0.9$), 1.7 ± 2 ($p < 0.001$, $d = 1.1$), and 27.9 ± 37.4 Gy·cm^2 ($P = 0.269$, $d = 0.1$), respectively. These corresponded to 76%, 88%, and 19% reductions in dose, respectively, when compared to Group I. The aortogram accounted for a mean of 10% of the total KAP across all 95 patients in Group II.

Table 3 shows the bivariate correlations using Pearson's correlations for Group II between all predictor variables and KAP. The following independent variables were statistically significant ($P < 0.01$): body mass, BMI, Ka, r, fluoroscopy time, total DSA, total CRM, and total fluoroscopy dose.

A Pearson's correlation matrix for the following variables is shown in Table 4: BMI, number of fibroids, total fibroid volume, total uterus volume, Ka, r, fluoroscopy time, total DSA dose, total CRM dose, and total fluoroscopy dose. A P-value < 0.01 was considered statistically significant.

The MLR model revealed that total fluoroscopy dose, Ka, r, and total uterus volume were significant ($P < 0.05$) predictors of KAP and in total accounted for 96.3% of the variance (Table 5). The analysis demonstrated that 88.2% of the variance was accounted for by total fluoroscopy dose, a further 7.1% was accounted for when adding Ka, r, and a further 1% was accounted for when adding total uterus volume to the regression model. During the stepwise process, the following variables were excluded: BMI, total number of fibroids, total fibroid volume, fluoroscopy time, total DSA dose, and total CRM dose.

The regression model that identified the radiation dose predictor variables for UAE procedures performed on the upgraded angiography system was found to be:

$$KAP = 1.014(total\ fluoroscopy\ dose) + 80.556(Ka, r) + 0.015(total\ uterus\ volume)$$

where total fluoroscopy dose (95% CI (0.925, 1.103)), Ka, r (95% CI (66.881, 94.230)), and total uterus volume (95% CI (0.009, 0.021)) were measured in $Gy{\cdot}cm^2$, Gy, and cm^3, respectively.

Figure 1 shows the Bland-Altman plot of agreement between the Actual KAP and Predicted KAP values for Group II. The MLR model and variables were used to calculate the Predicted KAP. A one-sample T-test of the Difference (Actual KAP – Predicted KAP) produced a non-statistically significant result ($P > 0.001$) and therefore a Bland-Altman plot could be used. It was found that the mean difference was 0.39 $Gy{\cdot}cm^2$, and the LoA were +28.49 and -27.71 $Gy{\cdot}cm^2$. A linear regression between the Difference and Mean ([Actual KAP + Predicted

KAP]/2) was not statistically significant (P = 0.111, r^2 = 0.027) and thus illustrated no proportional bias. The regression equation was found to be $y = 0.4667x - 80$. The Bland-Altman plot also shows the readings as divided into three different BMI categories (18.5 ≤ BMI ≤ 24.9 kg/m^2, 25 ≤ BMI ≤ 29.9 kg/m^2, and BMI ≥ 30 kg/m^2. Additionally, the M ± SD Difference/Mean percentage error was -2.9 ± 22.5%.

4. Discussion

This study validated the novel, dose-limiting technology of the upgraded angiography system and its advanced capabilities by significantly reducing the radiation dose exposure to patients receiving UAE at our centre. A comparison of the preceding generation (Group I) and upgraded (Group II) angiography system demonstrated a reduction in KAP and Ka, r by 63% (143.2 Gy·cm^2 vs 52.9 Gy·cm^2; P < 0.001, d = 0.8) and 67% (0.6 Gy vs 0.2 Gy; P < 0.001, d = 0.8), respectively. We established a new regression model for the upgraded angiography system based on KAP, which identified total fluoroscopy dose, Ka, r, and total uterus volume as the key radiation dose predictors. The Bland-Altman plot revealed a high predictive accuracy of the MLR model and the identified radiation dose predictors. The mean difference was 0.39 Gy·cm^2 and the limits of agreement (LoA) were +28.49 and -27.71 Gy·cm^2, and thus demonstrated no proportional bias. This model differentiates from that which was found in our earlier study using the Allura system[(25)], since a new set of variables were inputted into the MLR (LIH dose information is not available on the Azurion system) and thereby introducing the concept of system-dependent regression models. In this study, UAE radiation dose exposure had been optimised by the proprietary dose-limiting algorithms on the upgraded angiography system to the extent that previously identified dose predictor variables such as total DSA and total CRM dose were no longer significant at a multivariable level. Radiation dose reduction was also achievable through the interventional radiologist and interventional radiographer’s application of dose optimisation techniques available on the upgraded angiography system.

The upgraded angiography system has the capacity to yield a wider dynamic range, with improved spatial resolution and decreased image lag.[(16-17)] These features allow for the system to effectively reach its radiation dose reduction potential, such that DSA and CRM imaging are no longer identified as radiation dose predictors in this study. The new radiation dose predictors from the system-dependent MLR model reveal that future UAE procedures require attentive use of intermittent fluoroscopy to reduce the overall Ka, r and subsequent skin entrance dose. Intermittent fluoroscopy should be minimised during uterine artery catheterisation and embolic injection. Total uterus volume, however, is an uncontrollable variable. The novel real-time processing technique (AlluraClarity, Philips Healthcare, The Netherlands) and the intra-procedural optimisation by the interventional radiologist and interventional radiographer (including reduced frame rates and avoidance of magnification) demonstrated a reduction in total DSA and total CRM dose by 76% and 88%, respectively.

There is a paucity of literature that pertains to the formulation of regression models for UAE or the optimisation of identified dose predictors from derived regression models. Scheurig-Muenkler et al[(26)] used regression analysis to determine the influence of BMI on the expected radiation dose which yielded a significant exponential association ($P < 0.01$). They formed a simplified equation to define the relationship between BMI and radiation dose (KAP).[(26)] Lacayo et al[(32)] found that the strongest correlation among the radiation dose measures compared were between cumulative dose (i.e., Ka, r) and BMI ($r = 0.070$). However, in our study KAP was used as the dependent variable since this parameter represents the total energy incident on the patient and can be used to calculate effective dose to determine stochastic risks.[(33)] Furthermore, a recent study by Soliman et al [(27)] used multivariable logistic regression analysis to ascertain which independent prognostic variables could provide an estimate of the likelihood of obtaining a high KAP value. Their regression model was formed as follows: *Logit(KAP) = -6.1525 + 0.0416(Fluoroscopy time) + 0.1028(number of images) + 0.1675(BMI) – 0.1012(Experience of interventional radiologists)*.[(27)] Some of the notable differences between the study by Soliman et al[(27)] and our study is that a bi-plane angiography system was used, and a different set of variables were inputted into a non-linear regression analysis. BMI was found to be a common significant predictor variable across the three studies[(26,27,32)], however was not a significant factor in our MLR model. BMI was significant on a bivariate level with Ka,r ($P < 0.001$), fluoroscopy time ($P = 0.006$), and total fluoroscopy dose ($P < 0.001$). Due to the differences in the methodology, statistical analyses, and dose predictor variables used by these studies[(26,27,32)], these regression models could not be applied to the UAE practice at our centre.

This study presents new radiation dosimetry data on the upgraded angiography system where significant dose reductions have been attained during UAE. Currently, there is no known literature on UAE radiation dose using the Azurion 7 M20 with FlexArm (Philips Healthcare, Eindhoven, Netherlands) which at the time of this study, uses advanced technology equipped with hardware and software adjustments that synergise image processing to reduce dose without impairing image quality. Scheurig-Muenkler et al[26] suggested that the use of modern angiography systems and strict application of dose reduction methodology led to a significantly lower radiation dose, and therefore the target KAP should be kept below 50 Gy·cm^2. The reported dose reductions in this study for KAP (M = 52.9 Gy·cm^2; median = 30.6 Gy·cm^2) and Ka, r (M = 0.2 Gy; median = 0.14 Gy) are considerably lower than the mean values from previous studies where an upgraded angiography system was used, such as Durrani et al[34] (KAP = 206 Gy·cm^2), Schernthaner et al[35] (KAP = 146 Gy·cm^2; Ka, r = 0.6 Gy), Thomaere et al[36] (KAP = 102 Gy·cm^2; Ka, r not reported), Kohlbrenner et al[37] (KAP = 175 Gy·cm^2; Ka, r = 1.1 Gy), Sapoval et al[38] (KAP = 146 Gy·cm^2 and Ka, r = 0.6 Gy), and Mondshine et al[39] (KAP = 146 Gy·cm^2; Ka, r = 0.8 Gy). The Azurion 7 M20 with FlexArm features ClarityIQ (Philips Healthcare, Eindhoven, Netherlands), which allows for achieving clear angiographic visibility at low x-ray dose levels for patients of different sizes. This is functionally possible through the novel real-time processing of spatial filtering and temporal noise reduction algorithms, where motion compensation and pixel averaging of large areas of noise occurs allowing for less radiation dose for similar image quality.[19] Additionally, the technology is equipped with an optimised acquisition chain including the grid switch, beam filtering, pulse width, spot size, detector, and image processing engine.[15] Dose optimisation techniques used by the interventional radiographer included active collimation, avoidance of geometric magnification (using digital magnification instead) or change of detector field (48cm), APC (automatic position control) without radiation for table and tube position recall, live contrast/brightness/edge enhancement, and reduced DSA acquisition frame rates. Interventional radiologist and interventional radiographer's level of familiarisation of system capabilities is critical to achieve the maximal potential of dose optimisation.

A limitation for this study was that the regression model adopted from the previous publication[25] was unable to predict the total KAP since an independent variable (total LIH dose) from the equation was not available from this machine as it was previously. The stored fluoroscopy information is no longer saved on the Azurion system's dose report and LIH was not used as a roadmap during the UAE procedures, thereby implicating possible further dose reductions. Another limitation was that the estimated organ doses for the ovaries and uterus, as well as the effective dose were not calculated for the patients from both groups. Studies by Vetter et al[40], Sapoval et al[41], and Nikolic et al[42] have shown that ovarian doses are lowered even when the total DSA component were not omitted from use during UAE, but are reduced in frame rate, frequency of pulses, and dose rate. Future studies should explore the effects of optimising the two identified, controllable dose predictor variables, total fluoroscopy dose and Ka, r. Moreover, further investigations on the transferability of our findings and the use of the regression equation at other centres to achieve similar radiation dose reductions are recommended.

5. Conclusion

At an Australian radiology department, this study confirmed significant radiation dose reductions for patients having UAE procedures with the use of the upgraded angiography system. Our findings establish a standard for UAE radiation dosimetry in the Australian context. The development of a new system-dependent MLR model can be implemented at other centres performing UAE on the upgraded angiography system and thus benefit radiation dose practices and allow for the reproducibility of our results by optimising known radiation dose predictors.

Acknowledgement

The authors would like to thank the Interventional Radiology team at SAN Radiology & Nuclear Medicine, Sydney Adventist Hospital for their support and efforts in data collection for this study.

References

1. Liang E, Brown B, Kirsop R, Stewart P, Stuart A. Efficacy of uterine artery embolisation for treatment of symptomatic fibroids and adenomyosis - an interim report on an Australian experience. Aust N Z J Obstet Gynaecol. 2012 Apr;52(2):106–12.
2. Liang E, Brown B, Rachinsky M. A clinical audit on the efficacy and safety of uterine artery embolisation for symptomatic adenomyosis: Results in 117 women. Aust N Z J Obstet Gynaecol. 2018;58(4):454–9.
3. Ma J, Brown B, Liang E. Long-term durability of uterine artery embolisation for treatment of symptomatic adenomyosis. Aust N Z J Obstet Gynaecol [Internet]. [cited

2021 Mar 3]. Available from: https://obgyn.onlinelibrary.wiley.com/doi/abs/10.1111/ajo.13304

4. Gupta JK, Sinha A, Lumsden MA, Hickey M. Uterine artery embolization for symptomatic uterine fibroids. Cochrane Database Syst Rev. 2014 Dec 26;(12):CD005073.
5. Spies JB, Frenk NE. Better Understanding Our Tools for Uterine Fibroid Embolization. Radiology. 2021 Feb;298(2):466–7.
6. Lyon SM, Cavanagh K. Uterine artery embolisation - a treatment alternative for women with fibroids. Aust Fam Physician. 2006 May;35(5):300–3.
7. Clements W, Ang WC, Law M, Goh GS. Treatment of symptomatic fibroid disease using uterine fibroid embolisation: An Australian perspective. Australian and New Zealand Journal of Obstetrics and Gynaecology. 2020;60(3):324–9.
8. Nocum DJ, Robinson J, Liang E, Thompson N, Reed W. The factors contributing to the total radiation exposure of patients during uterine artery embolisation. J Med Radiat Sci. 2019;66(3):200–11.
9. The 2007 Recommendations of the International Commission on Radiological Protection. ICRP publication 103. Ann ICRP. 2007;37(2–4):1–332.
10. Manyonda I, Belli A-M, Lumsden M-A, Moss J, McKinnon W, Middleton LJ, et al. Uterine-Artery Embolization or Myomectomy for Uterine Fibroids. N Engl J Med. 2020 Jul 30;383(5):440–51.
11. Ghanaati H, Sanaati M, Shakiba M, Bakhshandeh H, Ghavami N, Aro S, et al. Pregnancy and its Outcomes in Patients After Uterine Fibroid Embolization: A Systematic Review and Meta-Analysis. Cardiovasc Intervent Radiol. 2020 Aug;43(8):1122–33.
12. Equipment, Medicare and diagnostic imaging [Internet]. Australian Government Department of Health; [cited 2021 Oct 24]. Available from: https://www1.health.gov.au/internet/main/publishing.nsf/Content/capsensdihttps://www1.health.gov.au/internet/main/publishing.nsf/Content/capsensdi
13. RACGP - Changes to the capital sensitivity arrangements for diagnostic imaging equipment [Internet]. [cited 2021 Oct 24]. Available from: https://www.racgp.org.au/the-racgp/faculties/rural/advocacy-and-research/member-updates/changes-to-the-capital-sensitivity-arrangements
14. NHS England Funding: Injecting £200 million into Aged Asset Replacement [Internet]. NHS Supply Chain. [cited 2021 Oct 24]. Available from:

https://www.supplychain.nhs.uk/news-article/nhs-england-funding-injecting-200-million-into-aged-asset-replacement/
15. Söderman M, Holmin S, Andersson T, Palmgren C, Babic D, Hoornaert B. Image noise reduction algorithm for digital subtraction angiography: clinical results. Radiology. 2013 Nov;269(2):553–60.
16. van Strijen MJ, Grünhagen T, Mauti M, Zähringer M, Gaines PA, Robinson GJ, et al. Evaluation of a Noise Reduction Imaging Technology in Iliac Digital Subtraction Angiography: Noninferior Clinical Image Quality with Lower Patient and Scatter Dose. J Vasc Interv Radiol. 2015 May;26(5):642-650.e1.
17. Studzińska E, Staniszewska MA. Impact of Allura Clarity Technology on Radiation Dose Exposure During Left Atrial Appendage Closure. Pol J Radiol. 2017;82:598–602.
18. Kastrati M, Langenbrink L, Piatkowski M, Michaelsen J, Reimann D, Hoffmann R. Reducing Radiation Dose in Coronary Angiography and Angioplasty Using Image Noise Reduction Technology. Am J Cardiol. 2016 Aug 1;118(3):353–6.
19. Haak RFF van den, Hamans BC, Zuurmond K, Verhoeven B a. N, Koning OHJ. Significant Radiation Dose Reduction in the Hybrid Operating Room Using a Novel X-ray Imaging Technology. Eur J Vasc Endovasc Surg. 2015 Oct 1;50(4):480–6.
20. Schernthaner RE, Duran R, Chapiro J, Wang Z, Geschwind J-FH, Lin M. A new angiographic imaging platform reduces radiation exposure for patients with liver cancer treated with transarterial chemoembolization. Eur Radiol. 2015 Nov;25(11):3255–62.
21. Wen X, Jiang X, Li R, Zhang J, Yang P, Shen B. Novel X-Ray Imaging Technology Allows Substantial Patient Radiation Reduction without Image Quality Impairment in Repetitive Transarterial Chemoembolization for Hepatocellular Carcinoma. Acad Radiol. 2015 Nov 1;22:1361–7.
22. Söderman M, Mauti M, Boon S, Omar A, Marteinsdóttir M, Andersson T, et al. Radiation dose in neuroangiography using image noise reduction technology: a population study based on 614 patients. Neuroradiology. 2013 Nov;55(11):1365–72.
23. Miller DL, Balter S, Cole PE, Lu HT, Schueler BA, Geisinger M, et al. Radiation doses in interventional radiology procedures: the RAD-IR study: part I: overall measures of dose. J Vasc Interv Radiol. 2003 Jun;14(6):711–27.
24. Kwon D, Little MP, Miller DL. Reference air kerma and kerma-area product as estimators of peak skin dose for fluoroscopically guided interventions. Med Phys. 2011 Jul;38(7):4196–204.

25. Nocum DJ, Robinson J, Halaki M, Liang E, Thompson N, Moscova M, et al. Identifying predictors of patient radiation dose during uterine artery embolisation. J Med Radiat Sci. 2021 Jun;68(2):131-8.
26. Scheurig-Muenkler C, Powerski MJ, Mueller J-C, Kroencke TJ. Radiation exposure during uterine artery embolization: effective measures to minimize dose to the patient. Cardiovasc Intervent Radiol. 2015 Jun;38(3):613–22.
27. Soliman K, Almutairi A, AlHarbi M, Almutairi K, Almutairi T, Bakkari M. Analysis of Factors Affecting Air Kerma Area Product Obtained during Uterine Artery Embolization Procedures Using Logistic Regression. Indian J Radiol Imaging [Internet]. 2021 Jul 28 [cited 2021 Aug 10]; Available from: http://www.thieme-connect.de/DOI/DOI?10.1055/s-0041-1733814
28. Nocum DJ, Robinson J, Halaki M, Båth M, Mekiš N, Liang E, et al. Uterine Artery Embolisation: Continuous Quality Improvement Reduces Radiation Dose While Maintaining Image Quality. Radiat Prot Dosimetry [Internet]. 2021 Sep 30 [cited 2021 Oct 12];(ncab145). Available from: https://doi.org/10.1093/rpd/ncab145
29. Cura M, Cura A, Bugnone A. Role of magnetic resonance imaging in patient selection for uterine artery embolization. Acta Radiol. 2006 Dec;47(10):1105–14.
30. Cohen J. Statistical Power Analysis for the Behavioral Sciences, 2nd Edn. Mahwah, NJ: Erlbaum. 1988.
31. Bland JM, Altman DG. Statistical methods for assessing agreement between two methods of clinical measurement. Lancet. 1986 Feb 8;1(8476):307–10.
32. Lacayo EA, Khera SS, Spies JB. Impact of Patient and Procedure-Related Factors on Radiation Exposure from Uterine Artery Embolization. Cardiovasc Intervent Radiol. 2020 Jan;43(1):120–6.
33. Schultz FW, Zoetelief J. Dose conversion coefficients for interventional procedures. Radiat Prot Dosimetry. 2005 Dec 1;117(1–3):225–30.
34. Durrani RJ, Fischman AM, van der Bom IMJ, Kim E, Nowakowski FS, Patel RS, et al. Radiation dose reduction utilizing noise reduction technology during uterine artery embolization: a pilot study. Clin Imaging. 2016 Jun;40(3):378–81.
35. Schernthaner RE, Haroun RR, Nguyen S, Duran R, Sohn JH, Sahu S, et al. Characteristics of a New X-Ray Imaging System for Interventional Procedures: Improved Image Quality and Reduced Radiation Dose. Cardiovasc Intervent Radiol. 2018 Mar;41(3):502–8.

36. Thomaere E, Dehairs M, Laenen A, Mehrsima A, Timmerman D, Cornelissen S, et al. A new imaging technology to reduce the radiation dose during uterine fibroid embolization. Acta Radiol. 2018 Dec 1;59(12):1446–50.
37. Kohlbrenner R, Kolli KP, Taylor AG, Kohi MP, Lehrman ED, Fidelman N, et al. Radiation Dose Reduction during Uterine Fibroid Embolization Using an Optimized Imaging Platform. J Vasc Interv Radiol. 2017 Aug;28(8):1129-1135.e1.
38. Sapoval M, Pellerin O, Rehel J-L, Houdoux N, Rahmoune G, Aubert B, et al. Uterine artery embolization for leiomyomata: optimization of the radiation dose to the patient using a flat-panel detector angiographic suite. Cardiovasc Intervent Radiol. 2010 Oct;33(5):949–54.
39. Mondshine R, Charles H, Aquino T, Clark T. Abstract No. 145: Radiation Dose of Uterine Fibroid Embolization Using a Flat Panel Digital Subtraction Angiography System. J Vasc Interv Radiol. 2008 Feb 1;19(2):S56.
40. Vetter S, Schultz FW, Strecker E-P, Zoetelief J. Patient radiation exposure in uterine artery embolization of leiomyomata: calculation of organ doses and effective dose. Eur Radiol. 2004 May;14(5):842–8.
41. Sapoval M, Pellerin O, Rehel J-L, Houdoux N, Rahmoune G, Aubert B, et al. Uterine artery embolization for leiomyomata: optimization of the radiation dose to the patient using a flat-panel detector angiographic suite. Cardiovasc Intervent Radiol. 2010 Oct;33(5):949–54.
42. Nikolic B, Spies JB, Campbell L, Walsh SM, Abbara S, Lundsten MJ. Uterine artery embolization: reduced radiation with refined technique. J Vasc Interv Radiol. 2001 Jan;12(1):39–44.

Tables

Table 1.

Descriptive statistics on demographic and clinical information and paired samples test between Group I and Group II

	Group I (Allura; 2010-2019)	**Group II (Azurion; 2020-*Present*)**	**Paired Samples Test**
Demographic and clinical information	**M ± SD (n = 95)**	**M ± SD (n = 95)**	***P*-value, Cohen's *d***
Age (years)	44.1 ± 6	43 ± 6	P = 0.262, d = 0.1
Height (cm)	163 ± 6	163 ± 7	P = 0.536, d = 0.1
Body Mass (kg)	66.7 ± 12	69.9 ± 14	P = 0.080, d = 0.2
BMI (kg/m^2)	24.9 ± 4	26.3 ± 5	P = 0.026*, d = 0.2
Total number of fibroids (n)	2 ± 2[‡]	1 ± 2[§]	P < 0.001*, d = 0.4
Total fibroid volume (cm^3)	208.6 ± 265[‡]	174.4 ± 261[§]	P = 0.359, d = 0.1
Total uterus volume (cm^3)	540 ± 507	407.5 ± 421	P = 0.048*, d = 0.2

‡ 81 patients in the Group I with symptomatic fibroids (15 patients with symptomatic adenomyosis), § 53 patients in the Group II with symptomatic fibroids (42 patients with symptomatic adenomyosis), **P*-value < 0.05 was considered statistically significant.

Table 2. Descriptive statistics on radiation dose measurements and paired samples test between both patient groups

	Group I (Allura; 2010-2019)	Group II (Azurion; 2020-*Present*)	Paired Samples Test	
Radiation dose measurements	**Mean ± SD (n = 95)**	**Mean ± SD (n = 95)**	***P*-value, Cohen's *d***	**% reduction [†]**
KAP (Gy·cm^2)	143.2 ± 115	52.9 ± 52	$P < 0.001$* $d = 0.8$	63%
Ka, r (Gy)	0.6 ± 0.5	0.2 ± 0.2	$P < 0.001$* $d = 0.8$	67%
Fluoroscopy time (min)	13.5 ± 6	11.6 ± 5	$P = 0.017$* $d = 0.2$	14%
Total DSA dose (Gy·cm^2)	93.5 ± 75	22.9 ± 24	$P < 0.001$* $d = 0.9$	76%
Total CRM dose (Gy·cm^2)	13.9 ± 10.6	1.7 ± 2	$P < 0.001$* $d = 1.1$	88%
Total fluoroscopy dose (Gy·cm^2)	34.4 ± 46	27.9 ± 37.4	$P = 0.269$* $d = 0.1$	19%

[†] The percentage reduction was calculated using the formula: *% reduction = [(Group I – Group II)/(Group I)] x 100%*. **P*-value < 0.05 was considered statistically significant.

Table 3. Bivariate correlations for Group II between KAP and each independent variable

Independent variable	**Pearson's correlation**	***P*-value**
Age (years)	-0.150	0.878
Height (cm)	-0.006	0.954
Body mass (kg)	0.554	< 0.001*
BMI (kg/m^2)	0.580	< 0.001*
Number of fibroids (*n*)	0.006	0.951
Total fibroid volume (cm^3)	0.162	0.116
Total uterus volume (cm^3)	0.190	0.065
Ka, r (Gy)	0.703	< 0.001*
Fluoroscopy time (min)	0.341	< 0.001*
Total DSA dose ($Gy \cdot cm^2$)	0.745	< 0.001*
Total CRM dose ($Gy \cdot cm^2$)	0.227	0.027*
Total fluoroscopy dose ($Gy \cdot cm^2$)	0.910	< 0.001*

* *P*-value < 0.01 (2-tailed) was considered statistically significant.

Table 4. Pearson's correlation matrix

KAP	BMI	Number of fibroids	Total fibroid volume	Total uterus volume	Ka, r	Fluoro-scopy time	Total DSA dose	Total CRM dose	Total Fluoro-scopy dose
BMI	0	-0.008 (*P* = 0.936)	0.082 (*P* = 0.431)	0.037 (*P* = 0.722)	0.673 (*P* < 0.001)*	0.279 (*P* = 0.006)*	0.694 (*P* < 0.001)*	0.312 (*P* = 0.002)*	0.356 (*P* < 0.001)*
Number of fibroids	-0.08 (*P* = 0.936)	0	0.589 (*P* < 0.001)*	0.515 (*P* < 0.001)*	-0.002 (*P* = 0.985)	0.013 (*P* = 0.899)	0.085 (*P* = 0.412)	-0.007 (*P* = 0.948)	-0.044 (*P* = 0.673)
Total fibroid volume	0.082 (*P* = 0.431)	0.589 (*P* < 0.001)*	0	0.825 (*P* < 0.001)*	0.073 (*P* = 0.483)	-0.043 (*P* = 0.679)	0.304 (*P* = 0.003)*	0.048 (*P* = 0.647)	0.033 (*P* = 0.749)
Total uterus volume	0.037 (*P* = 0.722)	0.515 (*P* < 0.001)*	0.825 (*P* < 0.001)*	0	0.015 (*P* = 0.886)	-0.107 (*P* = 0.301)	0.265 (*P* = 0.010)*	0.115 (*P* = 0.267)	0.093 (*P* = 0.371)
Ka, r	0.673 (*P* < 0.001)*	-0.002 (*P* = 0.985)	0.073 (*P* = 0.483)	0.015 (*P* = 0.886)	0	0.617 (*P* < 0.001)*	0.748 (*P* < 0.001)*	0.266 (*P* = 0.009)*	0.494 (*P* < 0.001)*
Fluoro-scopy time	0.279 (*P* = 0.006)*	0.013 (*P* = 0.899)	-0.043 (*P* = 0.679)	-0.107 (*P* = 0.301)	0.617 (*P* < 0.001)*	0	0.309 (*P* = 0.002)*	0.196 (*P* = 0.057)	0.270 (*P* = 0.008)*
Total DSA dose	0.694 (*P* < 0.001)*	0.085 (*P* = 0.412)	0.304 (*P* = 0.003)*	0.265 (*P* = 0.010)*	0.748 (*P* < 0.001)*	0.309 (*P* = 0.002)*	0	0.119 (*P* = 0.252)	0.404 (*P* < 0.001)*
Total CRM dose	0.312 (*P* = 0.002)*	-0.007 (*P* = 0.948)	0.048 (*P* = 0.647)	0.115 (*P* = 0.267)	0.266 (*P* = 0.009)*	0.196 (*P* = 0.057)	0.119 (*P* = 0.252)	0	0.188 (*P* = 0.068)
Total Fluoro-scopy dose	0.356 (*P* < 0.001)*	-0.044 (*P* = 0.673)	0.033 (*P* = 0.749)	0.093 (*P* = 0.371)	0.494 (*P* < 0.001)*	0.270 (*P* = 0.008)*	0.404 (*P* < 0.001)*	0.188 (*P* = 0.068)	0

* *P*-value < 0.01 (2-tailed) was considered statistically significant.

Table 5. Multivariable linear regression (MLR) model summary and coefficients[a] for the upgraded angiography system (Group II)

					Change statistics			
Model	**R square**	**Adjusted R square**	**Std. error of estimate**	**R square change**	**F change**	**df1**	**df2**	***P*-value**
	0.964	0.963	14.357	0.010	24.394	1	92	< 0.001
	Unstandardised coefficients					**95.0% confidence interval for B**		
Model	**B**	**Std. error**	**Standardised coefficients beta**	**t**	***P*-value**	**Lower bound**	**Upper bound**	**Collinearity statistics VIF**
Total fluoroscopy dose	1.014	0.045	0.643	22.528	< 0.001*	0.925	1.103	2.073
Ka, r	80.558	6.885	0.341	11.700	< 0.001*	66.881	94.230	2.160
Total uterus volume	0.015	0.003	0.116	4.939	< 0.001*	0.009	0.021	1.394

* *P*-value < 0.05 was considered statistically significant.

Figures

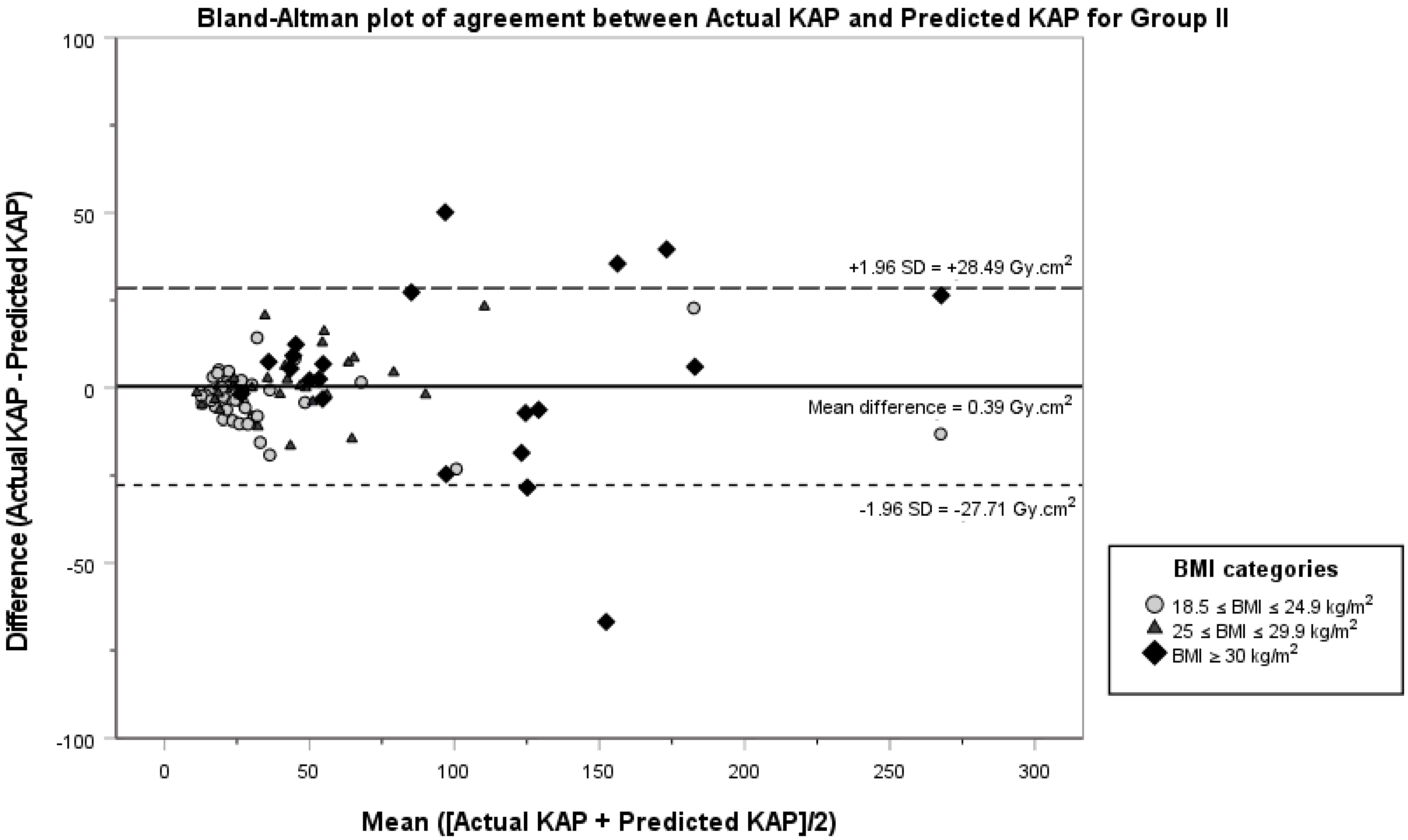

Bland-Altman plot of agreement between Actual KAP and Predicted KAP for Group II
100
50
0
-50
-100
Difference (Actual KAP - Predicted KAP)
0
50
100
150
200
250
300
Mean ([Actual KAP + Predicted KAP]/2)
+1.96 SD = +28.49 Gy.cm2
Mean difference = 0.39 Gy.cm2
-1.96 SD = -27.71 Gy.cm2
BMI categories
18.5 ≤ BMI ≤ 24.9 kg/m2
25 ≤ BMI ≤ 29.9 kg/m2
BMI ≥ 30 kg/m2

Figure 1. Bland-Altman plot for the comparison of the Actual KAP and Predicted KAP for Group II, with the representation of the limits of agreement (dotted lines), from -1.96 SD to +1.96 SD.